Nominally forbidden transitions in the interband optical spectrum of quantum dots

Gustavo A. Narvaez* and Alex Zunger†
National Renewable Energy Laboratory, Golden, Colorado 80401, USA
(Received 16 May 2006; published 18 July 2006)

We calculate the excitonic optical absorption spectra of (In,Ga)As/GaAs self-assembled quantum dots by adopting an atomistic pseudopotential approach to the single-particle problem followed by a configuration-interaction approach to the many-body problem. We find three types of *allowed* transitions that would be naively expected to be forbidden: (i) transitions that are parity forbidden in simple effective mass models with infinite confining wells (e.g., $1S$-$2S$, $1P$-$2P$) but are possible because of finite band offsets and orbital-mixing effects; (ii) light-hole-to-conduction-band transitions, enabled by the confinement of light-hole states; and (iii) transitions that show an enhanced intensity due to electron-hole configuration mixing with allowed transitions. We compare these predictions with results of eight-band $\mathbf{k}\cdot\mathbf{p}$ calculations as well as recent spectroscopic data. Transitions of types (i) and (ii) explain recently observed satellites of the allowed P-P transitions.

DOI: 10.1103/PhysRevB.74.045316 PACS number(s): 73.20.Mf, 73.22.−f, 73.43.Cd

I. INTRODUCTION

In quantum dot spectroscopy, rather simple, idealized theoretical approaches have been applied to discuss which confined interband optical transitions are formally allowed and which are formally forbidden. But one *expects* the simple rules not to work. Yet the mechanisms for failure have only been assessed within extensions of the simple models. To understand these mechanisms demands a high-level approach that naturally includes the complexity of the dots. Such approaches to the calculation of the optical properties are rare, with eight-band $\mathbf{k}\cdot\mathbf{p}$ calculations being among the most sophisticated approaches used so far.[1–6] Here, we discuss the nature of confined transitions in lens-shaped (In,Ga)As/GaAs quantum dots by using an atomistic pseudopotential-based approach.[7–9] Specifically, we study three mechanisms that render nominally forbidden transitions, in lower approximations, allowed transitions within more realistic approximations: (i) "$2S$-to-$1S$" and "$2P$-to-$1P$" "crossed" transitions allowed by finite band-offset effects and orbital mixing; (ii) transitions involving mixed heavy-hole and light-hole states, enabled by the confinement of light-hole states; and (iii) many-body configuration-mixing intensity enhancement enabled by electron-hole Coulomb interaction. We also compare our results with those of eight-band $\mathbf{k}\cdot\mathbf{p}$ calculations. Our atomistic pseudopotential theory explains recent spectroscopic data.

II. INTERBAND OPTICAL SPECTRUM OF (In,Ga)As/GaAs DOTS

A. Method of calculation

In our approach, the atomistic single-particle energies $\mathcal{E}_i$ and wave functions ψ_i are solutions to the atomistic Schrödinger equation[7]

$$\left(-\frac{1}{2}\nabla^2 + V_{SO} + \sum_{l,\alpha} v_\alpha(\mathbf{r}-\mathbf{R}_{l,\alpha})\right)\psi_i = \mathcal{E}_i\psi_i, \qquad (1)$$

where v_α is a pseudopotential for atoms of type α, with the lth site position $\mathbf{R}_{l,\alpha}$ in either the dot or the GaAs matrix. These positions are relaxed by minimizing the total elastic energy consisting of bond-bending plus bond-stretching terms via a valence force field functional.[9] This results in a realistic strain profile $\tilde{\varepsilon}(\mathbf{R})$ in the nanostructure.[10] In addition, v_α depends explicitly on the isotropic component of the strain $\mathrm{Tr}[\tilde{\varepsilon}(\mathbf{R})]$.[11] V_{SO} is a nonlocal (pseudo)potential that accounts for spin-orbit coupling.[9] In the single-particle approximation, the transition intensity for light polarized along $\hat{\mathbf{e}}$ is

$$I^{(SP)}(\omega;\hat{\mathbf{e}}) = \sum_{i,j} |\langle\psi_i^{(e)}|\hat{\mathbf{e}}\cdot\mathbf{p}|\psi_j^{(h)}\rangle|^2 \delta[\hbar\omega - \mathcal{E}_i^{(e)} + \mathcal{E}_j^{(h)}], \quad (2)$$

where $\mathbf{p}$ is the electron momentum.[12]

In addition to the single-particle effects, many-particle effects cause each of the monoexciton states $\Psi^{(\nu)}(X^0)$ to be a mixture of several electron-hole pair configurations (Slater determinants) e_ih_j; namely,

$$|\Psi^{(\nu)}(X^0)\rangle = \sum_{i,j} C_{i,j}^{(\nu)} |e_ih_j\rangle. \qquad (3)$$

The coefficients $C_{i,j}^{(\nu)}$ are determined by the degree of configuration mixing allowed by the electron-hole Coulomb and exchange interaction.[13] This mixing is determined by the symmetry of the e-h orbitals and by their single-particle energy separation. The many-body optical absorption for (incoherent) unpolarized light[14] is given by

$$I^{(MP)}(\hbar\omega) = \frac{1}{3}\sum_{\nu}\sum_{\hat{\mathbf{e}}=\hat{\mathbf{x}},\hat{\mathbf{y}},\hat{\mathbf{z}}} |M(\hat{\mathbf{e}})|^2 \delta[\hbar\omega - E^{(\nu)}(X^0)], \qquad (4)$$

where $M(\hat{\mathbf{e}}) = \langle\Psi^{(\nu)}(X^0)|\hat{\mathbf{e}}\cdot\mathbf{p}|0\rangle$. Thus, the configuration mixing can make transitions that are forbidden in the single-particle single-band approximation become allowed in the many-particle representation of Eq. (4) by borrowing oscillator strength from bright transitions.

B. Results

Figure 1 shows our calculated single-particle [Eq. (2); Fig. 1(a)] and many-particle [Eq. (4); Fig. 1(b)] absorption spectrum of X^0 for a lens-shaped $In_{0.6}Ga_{0.4}As/GaAs$ quan-

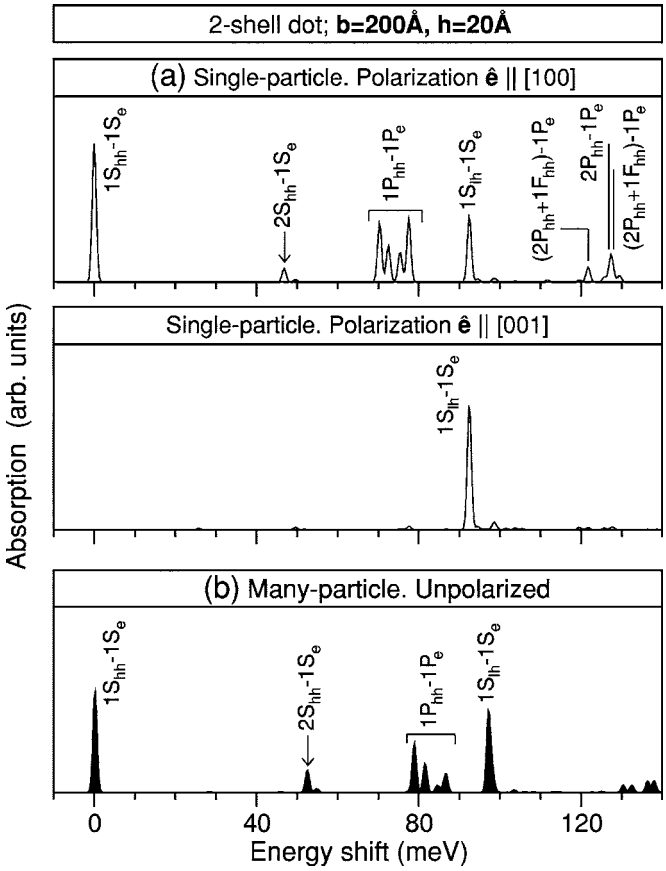

FIG. 1. Optical absorption spectrum of X^0 in a lens-shaped $In_{0.6}Ga_{0.4}As/GaAs$ quantum dot (base diameter $b=200$ Å, height $h=20$ Å) calculated (a) in the single-particle approximation [Eq. (2)] under in-plane ($\hat{\mathbf{e}}\|[100]$; top) and out-of-plane ($\hat{\mathbf{e}}\|[001]$; bottom) polarization; and (b) at the many-particle level [Eq. (4)] for unpolarized light. Energy is shown relative to (a) the single-particle gap $\mathcal{E}_0^{(e)}-\mathcal{E}_0^{(h)}=1333$ meV and (b) the ground-state energy $E^{(0)}(X^0)=1309$ meV of X^0.

tum dot with base diameter $b=200$ Å and height $h=20$ Å that confines two shells of electron states: $\{1S_e;1P_e\}$. The energy of the transitions is shown as a shift $\Delta\mathcal{E}$ from the single-particle exciton gap $\mathcal{E}_0^{(e)}-\mathcal{E}_0^{(h)}$ [in Fig. 1(a)] or the ground-state energy of the monoexciton $E^{(0)}(X^0)$ [in Fig. 1(b)]. Figure 2 shows equivalent results for two dots with $b=252$ Å and heights $h=20$ and 35 Å, which confine two $\{1S_e;1P_e\}$ and three $\{1S_e;1P_e;1D_e+2S_e\}$ shells of electron states, respectively.[15] As expected, we find nominally-allowed single-particle transitions, including (i) the fundamental transition $1S_{hh}$-$1S_e$ at $\Delta\mathcal{E}=0$ meV; (ii) the $1P_{hh}$-$1P_e$ transitions with energy shifts $\Delta\mathcal{E}\sim 75$ and 65 meV for dots with $b=200$ and 252 Å, respectively; and (iii) the transitions $1D_{hh}$-$1D_e$ and $2S_{hh}$-$2S_e$ at $\Delta\mathcal{E}\sim 130$ meV for the three-shell dot ($b=252$ Å, $h=35$ Å). Note that the underlying atomistic C_{2v} symmetry of the circular-base lens-shaped dot splits the electron and hole $1P$ and $1D$ states into three and five levels, respectively, and causes these states to be a mixture of $L_z=\pm 1$ and $L_z=\pm 2$, respectively. [L_z is the projection of the angular momentum along the cylindrical [001], out-of-plane) axis of the dot.] Thus, in contrast to predictions of simplified

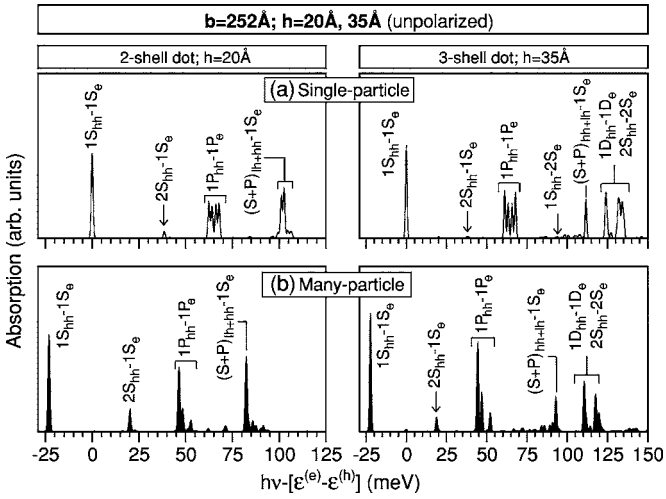

FIG. 2. *Idem* Fig. 1(b) for two $In_{0.6}Ga_{0.4}As/GaAs$ quantum dots that confine two (left panel) and three (right) shells of electron states, with heights $h=20$ and 30 Å, respectively, and base $b=252$ Å.

models that assume $C_{\infty v}$ shape symmetry, transitions involving states $1P$ and $1D$ are split into four and nine lines, respectively (Figs. 1 and 2). We next discuss the *nominally forbidden* transitions.

1. Band-offset- and orbital-mixing-induced 1S-2S transitions

If the electron and hole envelope wave functions are identical, the envelope-function selection rules indicate that only $\Delta i=0$ ($i\rightarrow i$) transitions are allowed, as assumed, e.g., in Refs. 16–20. This will be the case in the single-band effective mass approximation if the confinement potential (band offset between dot and environment) for electron and hole is infinite. In contrast, we find a few $\Delta i\neq 0$ transitions with significant intensity: (i) $2S_{hh}$-$1S_e$ [Figs. 1(a) and 2(a)], which we find *below* $1P_{hh}$-$1P_e$; (ii) four transitions that involve the electron states $1P_e$ and hole states $2P_{hh}$ (also found in Ref. 21) and $2P_{hh}+1F_{hh}$ [Fig. 1(a)]; and (iii) transitions $1S_{hh}$-$2S_e$, $2S_{hh}$-$1D_e$, and $1D_{hh}$-$2S_e$, in the three-shell dot (Fig. 2). There are two reasons why $\Delta i\neq 0$ transitions are allowed. First, in the case of *finite* band offsets or, equivalently, when the electron and hole wave functions are not identical, the condition $\Delta i=0$ is relaxed and transitions $j\rightarrow i$ may be allowed even in the effective mass approximation. The latter happens to be the case in the work of Vasanelli *et al.* (Ref. 21) in which $2S_{hh}$-$1S_e$ and $2P_{hh}$-$1P_e$ transitions between confined electron and hole levels were found to have finite, non-negligible oscillator strength. Second, orbital mixing also makes such transitions allowed: For example, a dot made of zinc-blende material and having a lens or cylindrical shape has the atomistic symmetry C_{2v} while spherical dots have T_d symmetry. In contrast, continuumlike effective-mass-based theories for dots use artificially higher symmetries. In fact, the ability of the envelope-function approximation to recognize the correct point-group symmetry depends on the number N of Γ-like bands used in the expansion.[22] $N=1$ corresponds to the "particle-in-a-box" or to the parabolic single-band effective mass approximation; $N=6$ corresponds to

including the valence-band maximum (VBM) states only; and $N=8$ corresponds to considering the VBM states plus the conduction-band minimum. Higher values of N have been also considered.[23,24] Thus, (a) within the $N=1$ single-band effective-mass approximation one uses the symmetry of the *macroscopic shape* (lens, cylinder, pyramid, sphere) rather than the true *atomistic* symmetry. For example, for zinc-blende lenses and cylinders one uses $C_{\infty v}$ symmetry rather than the correct C_{2v}. (b) The eight-band $\mathbf{k}\cdot\mathbf{p}$ Hamiltonian assumes cubic (O_h) symmetry to describe the electronic structure of the dots,[25] the resulting symmetry group is dictated by *both* the symmetry of the macroscopic shape and the cubic symmetry. In the case of square-pyramid-shaped dots the symmetry is C_{4v} rather than the correct C_{2v}.[26]

In single-band effective mass approaches, the transition i-j is allowed as long as the overlap between the respective envelope functions is nonzero. For example, for spherical quantum dots one expects S-S transitions to be allowed but not D-S transitions. Yet, in the true point-group symmetry of the *zinc-blende* sphere the highest occupied hole state has mixed $S+D$ symmetry, which renders transition $1S_h$-$1D_e$ allowed,[27,28] and similarly the "$2S$-$1S$" transition is allowed because the $2S_{hh}$ state also contains $1S_{hh}$ character.[29]

2. Strong light-hole–electron transitions

In *bulk* zinc-blende semiconductors the valence-band maximum is made of degenerate heavy-hole (hh, $|3/2,\pm 3/2\rangle$) and light-hole (lh, $|3/2,\pm 1/2\rangle$) states.[30] While both optical transitions hh-Γ_{1c} and lh-Γ_{1c} are polarized in the $\hat{\mathbf{x}}$-$\hat{\mathbf{y}}$ plane, only the latter transition presents polarization along $\hat{\mathbf{z}}$ ($\parallel[001]$). Under biaxial strain these hh and lh states split. In bulk the relative energy of these states and their splitting depend on the strain: for compressive strain (e.g., InAs on GaAs) the lh is below the hh while for tensile strain (e.g., GaAs on InAs) the lh is above the hh.[31] In *quantum dots* the energy of lh states is unknown. More importantly, it is generally assumed to be unconfined; so the lh-Γ_{1c} transition is expected to be absent from spectroscopic data. Nonetheless, Minnaert *et al.*[32] have speculated that despite the compressive strain in InAs/GaAs dots the lh state is above the hh states, while Ribeiro *et al.*[33] have suggested the presence of a lh-derived state *below* the hh states by measuring photoreflectance and photoabsorption in (In,Ga)As/GaAs dots. Adler *et al.*[34] and Akimov *et al.*[35] have also suggested the presence of lh-derived transitions in photoluminescence excitation (PLE) experiments in InAs/GaAs and CdSe/ZnSe self-assembled quantum dots, respectively. In addition, based on a six-band $\mathbf{k}\cdot\mathbf{p}$ calculation, Tadić *et al.*[36] have predicted that in disk-shaped InP/$In_{0.51}Ga_{0.49}P$ dots the light-hole states are confined at the interface of the disk and become higher in energy than heavy-hole states as the thickness of the disk is increased.

We show in Fig. 3(a) the strain-modified valence-band offsets of a lens-shaped $In_{0.6}Ga_{0.4}As$/GaAs sample with $b=252$ Å and $h=20$ Å, calculated along a line normal to the dot base that pierces the dot through its center. The energy is presented relative to the GaAs VBM [E_v(GaAs) $=-5.620$ eV]. We find that inside the dot the heavy-hole potential is above the light-hole one, while outside this order is

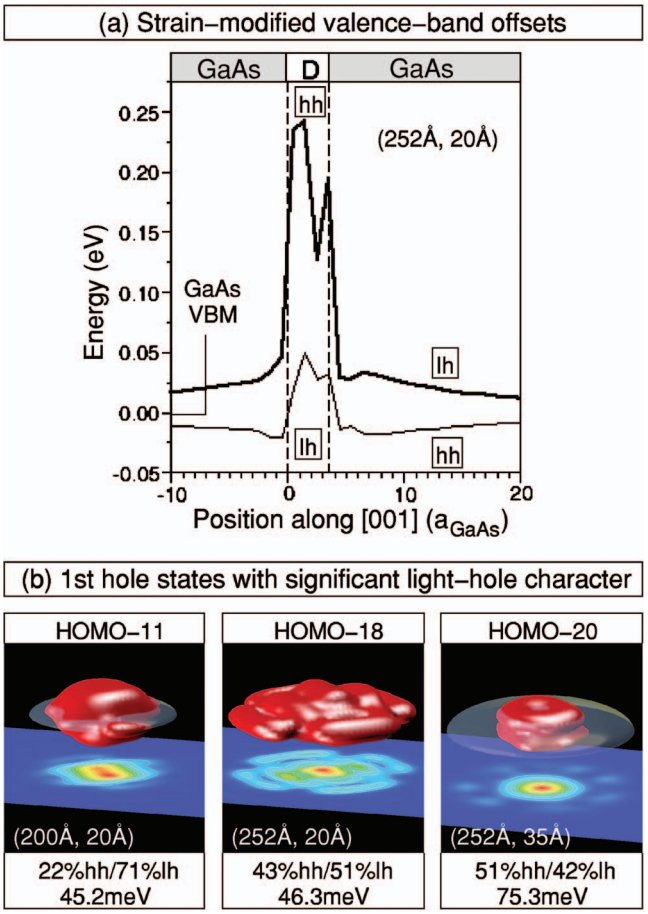

FIG. 3. (Color) (a) First (thick line) and second (thin line) strain-modified valence-band offsets along a line parallel to [001] that pierces a lens-shaped $In_{0.6}Ga_{0.4}As$/GaAs quantum dot through its center. The dot size is $b=252$ Å and $h=20$ Å. Position is measured in units of the lattice parameter of GaAs (a_{GaAs}) and the energies are relative to the GaAs VBM [E_v(GaAs)$=-5.620$ eV]. (b) Wave functions of the first hole state with significant lh character for different $In_{0.6}Ga_{0.4}As$/GaAs dots. Isosurfaces enclose 75% of the charge density, while contours are taken at 1 nm above the base. The energy $\mathcal{E}_j^{(h)}-E_v$(GaAs) of the state appears in each panel.

reversed; although the lh character of the lower-energy band offset leaks slightly into the barrier close to the dot. Because the dot is alloyed the band offsets inside the dot are jagged. In agreement with Ribeiro *et al.*,[33] but in contrast with Minnaert *et al.*,[32] our atomistic pseudopotential calculations reveal weakly confined light-hole states at energies deeper than the first hh state. The wave functions of the first of these states are shown in Fig. 3(b). The energy spacing between the highest hole state [HOMO ($\psi_0^{(h)}$)] and the deep lh-type states increases from 92.4 to 101.1 and 111.7 meV for HOMO−11 ($\psi_{11}^{(h)}$), HOMO−18 ($\psi_{18}^{(h)}$), and HOMO−20 ($\psi_{20}^{(h)}$), respectively. These states give raise to two lh-derived transitions in the absorption spectra: (i) $1S_{lh}$-$1S_e$ (Fig. 1) with the deep lh-type state being a mixture of 71% lh and 22% hh. As seen in Fig. 1, this transition has a large intensity in both $\hat{\mathbf{e}}\parallel[100]$ and $\hat{\mathbf{e}}\parallel[001]$ polarizations. (ii) $(S+P)_{lh+hh}$-$1S_e$ (Fig. 2) with hh (lh) percentages of 43 (51) and 51 (42) for the two-shell and three-shell dots, respectively. In these dots

with $b=252$ Å, the larger base size reduces the spacing between confined hole states and promotes character mixing. In the two-shell dot, the offset energy of this transition with respect to $1P_{hh}$-$1P_e$ is 36.0 meV, in excellent agreement with the observed value.[37] Note that simple models that follow the common assumption of unconfined lh states do not explain the observed feature.

3. Coulomb-induced transitions that are forbidden in the single-particle description

Due to the electron-hole Coulomb interaction, each monoexciton state $\Psi(X^0)$ is a mixture of electron-hole configurations [Eq. (3)]. This mix results in enhancement or diminishment of the intensity of both allowed and nominally forbidden transitions in the absorption spectra [Fig. 2(b)]. These are shown by comparing Fig. 1(a) vs Fig. 1(b) and Fig. 2(a) vs Fig. 2(b). The many-body effects include (i) enhancement of the intensity of the nominally forbidden transition $2S_{hh}$-$1S_e$ particularly in the 3-shell dot (Fig. 2); (ii) redistribution of the intensity of both the nominally allowed $1P_{hh}$-$1P_e$ transitions and the $1D_{hh}$-$1D_e$ and $2S_{hh}$-$2S_e$ transitions; and (iii) change of the intensity of the transitions involving deep hole states with significant light-hole character. The mixing enhancement $\eta(2S_{hh}\text{-}1S_e)=I^{(CI)}(2S_{hh}\text{-}1S_e)/I(2S_{hh}\text{-}1S_e)=3.2$ and $\eta(1S_{hh}\text{-}1S_e)=1.1$ for the 2-shell dot, while $\eta(2S_{hh}\text{-}1S_e)=8.2$ and $\eta(1S_{hh}\text{-}1S_e)=1.3$ for the three-shell dot. For both dots, the enhancement of transition $2S_{hh}$-$1S_e$ arises mainly from configuration mixing with the four configurations $|1P_{hh}1P_e\rangle$. The degree of mixing is small, ~2% for both dots, due to the large (~26 meV) energy splitting between these electron-hole configurations at the single-particle (noninteracting) level, yet sufficient to cause a sizable enhancement of the intensity. We find that the larger $\eta(2S_{hh}\text{-}1S_e)$ for the 3-shell dot arises from a larger mixing with configuration $|1S_{hh}1S_e\rangle$. *Comparison with experiment*: The calculated $2S_{hh}$-$1S_e$ transition is ~26 meV *below* the strongest $1P_{hh}$-$1P_e$ transition; in excellent agreement with those observed by Preisler *et al.*[37] in magnetophotoluminescence, who found 25 meV, and in contrast to the effective-mass approximation results of Vasanelli *et al.*, which place $2S_{hh}$-$1S_e$ *above* $1P_{hh}$-$1P_e$. The calculated $1S_{lh}$-$1S_e$ transition is 18.3 meV below $1P_{hh}$-$1P_e$, in only rough agreement with the value of 35 meV observed by Preisler *et al.*[37]

The effect of configuration mixing on the optical spectrum was previously discussed within the simplified single-band, two-dimensional effective mass (2D-EMA) parabolic model.[17,18] Such continuum theories assume macroscopic shapes that lead to significant degeneracies among the single-particle states of Eq. (1): P states are twofold degenerate; D states and $2S$ are degenerate; and the S-P and P-D energy spacings are equal. As a result, there is an artificially strong many-body mixing in Eq. (3). The many-particle exciton states with allowed Coulomb mixing are

$$|\Psi_A\rangle = |1S_{hh}1S_e\rangle,$$

$$|\Psi_B\rangle = \frac{1}{\sqrt{2}}(|1P_{hh}^{(+)}1P_e^{(+)}\rangle + |1P_{hh}^{(-)}1P_e^{(-)}\rangle),$$

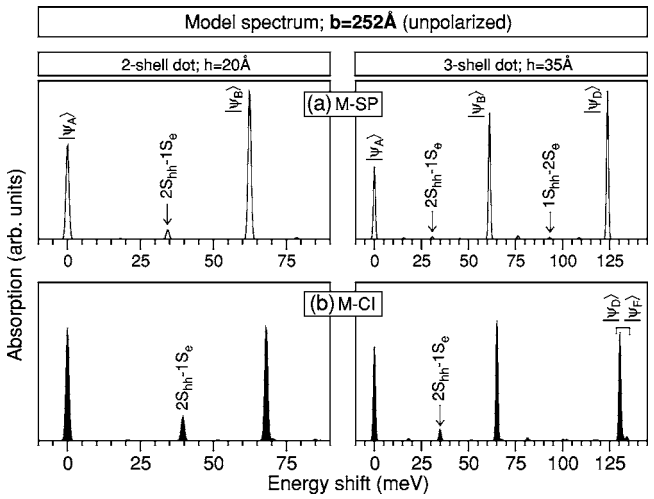

FIG. 4. Optical absorption spectrum of X^0 in two lens-shaped $In_{0.6}Ga_{0.4}As/GaAs$ quantum dots that confine two (left panel) and three (right) shells of electron states. In both cases, the spectra are calculated within a model single-particle (M-SP) [Eq. (2)] (a) and configuration-interaction (M-CI) approach [Eq. (4)] (b), assuming degenerate $1P$, $2D$, and $2S$ (in three-shell dot) electron and hole states but retaining the atomistic wave functions. Vertical scales are different for each dot.

$$|\Psi_H\rangle = \frac{1}{\sqrt{2}}(|2S_{hh}1S_e\rangle + |1S_{hh}2S_e\rangle),$$

$$|\Psi_D\rangle = \frac{1}{\sqrt{3}}(|1D_{hh}^{(+)}1D_e^{(+)}\rangle + |1D_{hh}^{(-)}1D_e^{(-)}\rangle + |2S_{hh}2S_e\rangle),$$

$$|\Psi_F\rangle = \frac{1}{\sqrt{6}}(|1D_{hh}^{(+)}1D_e^{(+)}\rangle + |1D_{hh}^{(-)}1D_e^{(-)}\rangle - 2|2S_{hh}2S_e\rangle). \quad (5)$$

Here, the $(\pm)$ labels indicate $L_z=\pm1$ and ±2 for the P and D states, respectively. The Coulomb interaction couples states $|\Psi_B\rangle$ and $|\Psi_H\rangle$. Thus the P-P transition is split into two lines $\Psi_a^{(s,p)} \simeq |\Psi_B\rangle + |\Psi_H\rangle$ and $\Psi_b^{(s,p)} \simeq |\Psi_B\rangle - |\Psi_H\rangle$. States $|\Psi_D\rangle$ and $|\Psi_F\rangle$, which arise from nominally allowed electron-hole configurations, are also coupled; consequently, the D-D transition splits into two lines $\Psi_a^{(d,d)} \simeq |\Psi_D\rangle + |\Psi_F\rangle$ and $\Psi_b^{(d,d)} \simeq |\Psi_D\rangle - |\Psi_F\rangle$. The mixing enhancement $\eta(|\psi_H\rangle)$ within this model is ∞ (because transitions $2S_{hh}$-$1S_e$ and $1S_{hh}$-$2S_e$ are *forbidden* at the single-particle level).

To compare our atomistic predictions with the model calculations, we *deliberately neglect* in the pseudopotential-based calculation the atomistic-induced splitting of the $1P$, and $1D$ and $2S$ states (but preserve their atomistically calculated wave functions). We calculate the absorption spectrum at the single-particle level [Eq. (2)] and separately in the many-particle approximation [Eq. (4)].[38,39] Figures 4(a) and 4(b) show, respectively, the atomistic model calculations of the *single-particle* and *many-particle* absorption spectra. By comparing the results of Fig. 4 (atomistic wave functions; no P or D splittings) with the expectations from Eq. (5) (continuum wave functions; no P or D splittings), we find that (i)

in the atomistic calculation the configuration-interaction-(CI-)enhanced transition corresponds to a mixture of states $|2S_{hh}1S_e\rangle$ and $|\Psi_B\rangle$ instead of a mixture of $|\psi_H\rangle$ and $|\psi_B\rangle$ as in the model of Eq. (5); and (ii) the *D*-shell transition peak [$|\psi_D\rangle$, Fig. 4(a)] splits into two transitions that correspond to a mixture of $|\psi_D\rangle$ and $|\psi_F\rangle$ as in the 2D-EMA model.

C. Comparison with eight-band k·p calculations of the interband optical spectrum

Other authors have calculated the absorption spectrum of pure, nonalloyed InAs/GaAs quantum dots using the eight-band **k·p** method with cubic symmetry. A comparison with our atomistic, pseudopotential-based predictions in alloyed (In,Ga)As/GaAs dots shows the following main features.

(i) Our prediction of transition $2S_{hh}$-$1S_e$ between 1*S*-1*S* and 1*P*-1*P* is consistent with the findings of nominally forbidden transitions between 1*S*-1*S* and 1*P*-1*P* by Heitz *et al.*,[1] who calculated the (many-body) absorption spectrum of a monoexciton in pyramid-shaped nonalloyed InAs/GaAs dots with base length of $d=170$ Å (height unspecified); Guffarth *et al.*,[2] who calculated the (many-body) absorption spectra of truncated-pyramid InAs/GaAs dots ($d=180$ Å, $h=35$ Å); and the single-particle calculations of Sheng and Leburton[3] in the case of a pure nonalloyed lens-shaped InAs/GaAs dot with $d=153$ Å and $h=34$ Å. Conversely, other eight-band **k·p** plus CI calculations did not predict nominally-forbidden transitions between 1*S*-1*S* and 1*P*-1*P*, like those of Stier *et al.*[4] for a truncated-pyramid InAs/GaAs dot with height $h=34$ Å (base length unspecified), who found three groups of transitions: 1*S*-1*S*, 1*P*-1*P*, and 1*D*-1*D*, *without* the presence of satellites around transitions 1*P*-1*P*. Similarly, recent calculations by Heitz *et al.*[5] of the absorption spectrum for small, flat ($d=136$ Å and heights from 3–7 monolayers) truncated-pyramid InAs/GaAs dots also predicted the *absence* of nominally forbidden transitions between 1*S*-1*S* and 1*P*-1*P*.

(ii) We predict that transitions 1*P*-1*P* and 1*D*-1*D* are split and span about 10 and 15 meV, respectively. Instead, the **k·p**-based calculations of Heitz *et al.*[1] predict that 1*P*-1*P* and 1*D*-1*D* transitions are much more heavily split, each group spanning about 50 meV.

(iii) Sheng and Leburton[6] calculated the single-particle dipole oscillator strength for a truncated-pyramid InAs/GaAs dot with $d=174$ Å and $h=36$ Å and found strong nominally forbidden transitions 1*D*-1*P* nearly 50 meV above transitions 1*P*-1*P*, and a transition HOMO−7 to 2*S*. Our predictions differ from these in that we find transitions $(2P_{hh}+1F_{hh})$-$1P_e$ above 1*P*-1*P* [Fig. 1(a)]. In addition, in this energy interval (~50 meV above 1*P*-1*P*) we do not predict hole states with nodes along the [001] axis of the dots.

(iv) None of the eight-band **k·p**-based plus CI calculations of Refs. 1, 2, 4, and 5 predicted strong light-hole-to-conduction-band transitions originating from deep, weakly confined hole states with predominant lh character lying between the 1*P*-1*P* and 1*D*-1*D* transitions.

III. CONCLUSION

Atomistic, pseudopotential-based calculations of the excitonic absorption of lens-shaped (In,Ga)As/GaAs quantum dots predict nontrivial spectra that show nominally forbidden transitions allowed by single-particle band-offset effects as well as enhanced by many-body effects, and transitions involving deep, weakly confined hole states with significant light-hole character. These transitions explain the satellites of the *P*-*P* nominally allowed transitions recently observed in PLE.

ACKNOWLEDGMENTS

The authors thank G. Bester and L. He for valuable discussions, and V. Preisler (ENS, Paris) for making data in Ref. 37 available to them prior to publication. This work was funded by U.S. DOE-SC-BES-DMS, under Contract No. DE-AC3699GO10337 to NREL.

*Email address: g_a_narvaez@hotmail.com
†Email address: alex_zunger@nrel.gov

[1] R. Heitz, O. Stier, I. Mukhametzhanov, A. Madhukar, and D. Bimberg, Phys. Rev. B **62**, 11017 (2000).
[2] F. Guffarth, R. Heitz, A. Schliwa, O. Stier, M. Geller, C. M. A. Kapteyn, R. Sellin, and D. Bimberg, Phys. Rev. B **67**, 235304 (2003).
[3] W. Sheng and J.-P. Leburton, Phys. Status Solidi B **237**, 394 (2003).
[4] O. Stier, R. Heitz, A. Schliwa, and D. Bimberg, Phys. Status Solidi A **190**, 477 (2002).
[5] R. Heitz, F. Guffarth, K. Pötschke, A. Schliwa, D. Bimberg, N. D. Zakharov, and P. Werner, Phys. Rev. B **71**, 045325 (2005).
[6] W. Sheng and J.-P. Leburton, Appl. Phys. Lett. **80**, 2755 (2002).
[7] A. Zunger, Phys. Status Solidi B **224**, 727 (2001).
[8] L.-W. Wang and A. Zunger, Phys. Rev. B **59**, 15806 (1999).
[9] A. J. Williamson, L. W. Wang, and A. Zunger, Phys. Rev. B **62**, 12963 (2000).
[10] C. Pryor, J. Kim, L. W. Wang, A. J. Williamson, and A. Zunger, J. Appl. Phys. **83**, 2548 (1998).
[11] K. Kim, P. R. C. Kent, A. Zunger, and C. B. Geller, Phys. Rev. B **66**, 045208 (2002), and references therein.
[12] P. Y. Yu and M. Cardona, *Fundamentals of Semiconductors—Physics and Materials Properties* (Springer, Berlin, 2003).
[13] A. Franceschetti, H. Fu, L. W. Wang, and A. Zunger, Phys. Rev. B **60**, 1819 (1999).
[14] Unpolarized photons incoming from all directions.
[15] G. A. Narvaez, G. Bester, and A. Zunger, J. Appl. Phys. **98**, 043708 (2005).
[16] U. Woggon, *Optical Properties of Semiconductor Quantum Dots* (Springer-Verlag, Berlin, 1997).
[17] G. A. Narvaez and P. Hawrylak, Phys. Rev. B **61**, 13753 (2001).
[18] P. Hawrylak, G. A. Narvaez, M. Bayer, and A. Forchel, Phys. Rev. Lett. **85**, 389 (2000).
[19] F. Findeis, A. Zrenner, G. Böhm, and G. Abstreiter, Solid State Commun. **114**, 227 (2000).

[20] U. Honester, R. Di Felice, E. Molinari, and F. Rossi, Appl. Phys. Lett. **75**, 3449 (1999).
[21] A. Vasanelli, R. Ferreira, and G. Bastard, Phys. Rev. Lett. **89**, 216804 (2002).
[22] A. Zunger, Phys. Status Solidi A **190**, 467 (2002).
[23] N. Rougemaille, H.-J. Drouhin, S. Richard, G. Fishman, and A. K. Schmid, Phys. Rev. Lett. **95**, 186406 (2005); C. W. Cheah, L. S. Tan, and G. Karunasiri, J. Appl. Phys. **91**, 5105 (2002); W. H. Lau, J. T. Olesberg, and M. E. Flatté, Phys. Rev. B **64**, 161301(R) (2001).
[24] S. Richard, F. Aniel, and G. Fishman, Phys. Rev. B **70**, 235204 (2004); **71**, 169901(E) (2005).
[25] C. Pryor, Phys. Rev. B **57**, 7190 (1998); W. Sheng and J.-P. Leburton, Phys. Status Solidi B **237**, 394 (2003).
[26] It is possible to have an eight-band $\mathbf{k}\cdot\mathbf{p}$ Hamiltonian for strained zinc-blende semiconductors with the correct tetrahedral (T_d) symmetry. [See H.-R. Trebin, U. Rössler, and R. Ranvaud, Phys. Rev. B **20**, 686 (1979).] If this Hamiltonian is used to find the electronic energy-level structure of a square-pyramid-shaped InAs/GaAs dot the symmetry of the problem is reduced to C_{2v}.
[27] J.-B. Xia, Phys. Rev. B **40**, 8500 (1989).
[28] H. Fu and A. Zunger, Phys. Rev. B **56**, 1496 (1997).
[29] Band-mixing effects mix the 1*S* and 2*S* character of the single-particle hole states.
[30] G. Bastard, *Wave Mechanics Applied to Semiconductor Heterostructures* (Halstead, New York, 1988).
[31] P. R. C. Kent, G. L. W. Hart, and A. Zunger, Appl. Phys. Lett. **81**, 4377 (2002).
[32] A. W. E. Minnaert, A. Yu. Silov, W. van der Vleuten, J. E. M. Haverkort, and J. H. Wolter, Phys. Rev. B **63**, 075303 (2001).
[33] E. Ribeiro, F. Cerdeira, M. J. S. P. Brasil, T. Heinzel, K. Ensslin, G. Medeiros-Ribeiro, and P. M. Petroff, J. Appl. Phys. **87**, 7994 (2000).
[34] F. Adler, M. Geiger, A. Bauknetch, F. Scholz, H. Schweizer, M. H. Pilkuhn, B. Ohnesorge, and A. Forchel, J. Appl. Phys. **80**, 4019 (1996).
[35] A. I. Akimov, A. Hundt, T. Flissikowski, P. Kratzert, and F. Henneberger, Physica E (Amsterdam) **17**, 31 (2003); T. Flissikowski, I. A. Akimov, A. Hundt, and F. Henneberger, Phys. Rev. B **68**, 161309(R) (2003).
[36] M. Tadić, F. M. Peeters, and K. L. Janssens, Phys. Rev. B **65**, 165333 (2002).
[37] V. Preisler, T. Grange, R. Ferreira, L. A. de Vaulchier, Y. Guldner, F. J. Teran, M. Potemski, and A. Lemaître, Phys. Rev. B **73**, 075320 (2006).
[38] Both dots confine more than three shells of hole states but we only consider three in this model calculation.
[39] In the pseudopotential-based plus CI calculation we do not use Eq. (5), but we let the Coulomb interaction mix the configurations $|e_i h_j\rangle$ that compose the monoexciton states [Eq. (3)]. We include the electron-hole direct Coulomb coupling but neglect the much smaller electron-hole exchange.